3D modelling of solute transport and mixing during managed aquifer recharge with an infiltration basin

Tidjani Bahar, Laurent Oxarango, Hélène Castebrunet, Yvan Rossier, Florian Mermillod-Blondin

Manuscript Details

Manuscript number CONHYD_2020_96

Title Three dimensional modeling of aquifer recharge with infiltration basins in urban area

Article type Research Paper

Abstract

In this paper, a 3D model of the vadose zone/aquifer system is implemented to simulate the fate of water and pollutants in storm water infiltration basin located in Chassieu (Lyon area, France). The geometry of the Django Reinhard experimental site was built from the DEM data of the National Geographic Institute (resolution of the digital elevation model is 1 m). The well-known Richards model is used to simulate the flow in the saturated and unsaturated zone of the study site. The transfer of solutes in the basin/aquifer system is modelled by the advection-dispersion-equation (ADE). The infiltration rate was calculated using a basin mass balance based on surface data (measured flowrate, water level in the basin and topography). In the first step, the calibration of the 3D groundwater flow model is carried out by comparison between observed and simulated piezometric levels. This calibration is based on a reference rainy episode chosen from the data measured by the OTHU. The results have shown a reasonable restitution of the measured data in view of the complexity of the real system. The calibrated set of parameters appeared suitable to simulate a period of 1 month presenting two significant rain events. The advection-dispersion-equation was then calibrated in order to reproduce the electrical conductivity decrease (intensity and dynamics) observed in control piezometers. The calibrated transport model was used to simulate the fate of a solute pollutant considered as a tracer. A characterization of the concentrations in control piezometers was carried out by post-treatment of the 3D calculation. Three main results were obtained: (1) 0 to 24% of the injection concentration could be recovered depending on the location of the piezometer around the basin with respect to the aquifer main flow direction, (2) the averaged concentration decreased by 40% if the measuring device is lowered by 5 m (effect of the depth) and (3) capillary trapping promotes a retention of up to 20% of the injected tracer in the vadose zone.

Keywords 3D modelling; MAR system; contaminant transport

Corresponding Author Bahar Tidjani Bahar

Corresponding Author's Institution University of Grenoble Alpes

Order of Authors Bahar Tidjani Bahar, Laurent Oxarango, Helene Castebrunet, Yvan Rossier, Florian Mermillod-Blondin

Suggested reviewers Joanne Vanderzalm, Joaquin Jimenez-Martinez, laurent lassabatere

Submission Files Included in this PDF

File Name [File Type]

Cover_letter_editor_JCH.docx [Cover Letter]

Paper_Manuscrit_Final.docx [Manuscript File]

conflit_of_interest_JCH.docx [Conflict of Interest]

Submission Files Not Included in this PDF

File Name [File Type]

Figure 1.PNG [Figure]

Figure 2.PNG [Figure]

Figure 3.png [Figure]

Figure 4.png [Figure]

Figure 5.png [Figure]

Figure 6.png [Figure]

Figure 7.png [Figure]

Figure 8.png [Figure]

Figure 9.png [Figure]

Figure 10.PNG [Figure]

Figure 11.PNG [Figure]

Figure 12.PNG [Figure]

Bahar Tidjani
Université Grenoble Alpes, CNRS
tidjanibahar@yahoo.fr

Grenoble
March 14th, 2020

Editor
Journal of Contaminant Hydrology

Dear Editor,

We are submitting our manuscript entitled 'Three dimensional modeling of aquifer recharge with infiltration basins in urban area' by T. Bahar, L. Oxarango, H. Castebrunet, Y. Rossier and F.M Blondin for consideration for publication in *Journal of Contaminant hydrology* and in the framework of GQ2019 special issue. As announced by GQ 2019 chairmans, we have a possibility to publish for this GQ special issue and our oral presentation intituled (reference number 302) ' 3d Modeling of Urban Grounwater Recharge from Stormwater Infiltration Basins'

Our paper presents a 3D model of the vadose zone/aquifer system in order to simulate the fate of water and pollutants in storm water infiltration basin located in Chassieu (Lyon area, France).

Please do not hesitate to contact us if you have any questions regarding our manuscript.

Best regards,

Bahar Tidjani

Title: Three dimensional modeling of aquifer recharge with infiltration basins in urban area

Tidjani Bahar[a], Laurent Oxarango[a], Hélène Castebrunet[b], Yvan Rossier[a], Florian Mermillod-Blondin[c]

[a] Université Grenoble Alpes, CNRS, IRD, Grenoble INP, IGE, Grenoble F-38000, France

[b] University Lyon, INSA Lyon, DEEP, F-69621 Villeurbanne Cedex, France

[c] Univ Lyon, Université Claude Bernard Lyon 1, CNRS, ENTPE, UMR5023, Écologie des Hydrosystèmes Naturels et Anthropisés, Villeurbanne, F-69622, France

Abstract

In this paper, a 3D model of the vadose zone/aquifer system is implemented to simulate the fate of water and pollutants in storm water infiltration basin located in Chassieu (Lyon area, France). The geometry of the Django Reinhard experimental site was built from the DEM data of the National Geographic Institute (resolution of the digital elevation model is 1 m). The well-known Richards model is used to simulate the flow in the saturated and unsaturated zone of the study site. The transfer of solutes in the basin/aquifer system is modelled by the advection-dispersion-equation (ADE). The infiltration rate was calculated using a basin mass balance based on surface data (measured flowrate, water level in the basin and topography). In the first step, the calibration of the 3D groundwater flow model is carried out by comparison between observed and simulated piezometric levels. This calibration is based on a reference rainy episode chosen from the data measured by the OTHU. The results have shown a reasonable restitution of the measured data in view of the complexity of the real system. The calibrated set of parameters appeared suitable to simulate a period of 1 month presenting two significant rain events. The advection-dispersion-equation was then calibrated in order to reproduce the electrical conductivity decrease (intensity and dynamics) observed in control piezometers. The calibrated transport model was used to simulate the fate of a solute pollutant considered as a tracer. A characterization of the concentrations in control piezometers was carried out by post-treatment of the 3D calculation. Three main results were obtained: (1) 0 to 24% of the injection concentration could be recovered depending on the location of the piezometer around the basin with respect to the aquifer main flow direction, (2) the averaged concentration decreased by 40% if the measuring device is lowered by 5 m (effect of the depth) and (3) capillary trapping promotes a retention of up to 20% of the injected tracer in the vadose zone.

Keywords: 3D modelling, MAR system, contaminant transport

I-Introduction

Managed aquifer recharge with storm water is largely used in urban areas because of their recognized hydraulic and hydrologic benefits (Bouwer, 2002; Dillon, 2005). The implementation of these practices contributes both at preventing flooding and at recharging aquifers (Davis et al., 2009; Hunt et al., 2010). The reuse of groundwater from urban artificial recharge is increasing in both emerging and developed countries to cope with the negative effects of climate change and rapid population growth (Bates et al., 2008). Nevertheless, urban development affects the quality of groundwater recharge (Bouwer, 2002; Maliva et al., 2006; Minskey et al.,2011). The urban groundwater can be contaminated by chemicals products, such as hydrocarbon, fuel-derivatives, heavy metals and nutrients, but also by pathogens and bacteria (Pitt et al., 1999). Consequently, these contaminants could increase the deterioration of groundwater quality and reduce at the same time the potential of infiltration basins to recharge aquifers (Tutulic et al., 2011). In addition, this impact on groundwater quality is strongly dependent on the hydrogeochemical characteristics of the aquifers and on the design and functioning of infiltration basins. Previous studies (Mason et al., 1999; Datry et al., 1999; Tedoldi et al., 2016) have shown that the vadose zone beneath the basin can play a major role in pollutant retention and biodegradation. However, quantifying the efficiency of these biochemical processes remains challenging. A major botleneck lies in the complexity of flow and transfers occurring in the vadose zone / aquifer continuum which plays a key role on the mobility of contaminants.

A detailed study of the lithology of the site under consideration in the present study was carried out by Goutaland et al. (2008). It exhibited a complex structure of the quaternary gravelly deposits at the metric and sub-metric scale. A subsequent theoretical study of flow and transport behaviour was proposed by Winiarski et al. (2013) involving a Mobile-Immobile model in order to deal with the heterogeneous nature of the soil. Nevertheless, such kind of model involves a large number of parameters. Thus, its application and validation at larger scale remains questionable. Even in well instrumented sites, the monitoring set-up generally consists in punctual data concerning the basin and the aquifer. Classical hydraulic data measurements consist in monitoring injected flowrate, water levels in the basin, hydraulic head in piezometers located around the basin. The water chemistry could be monitored using temperature, electric conductivity, dissolved oxygen, and pH probes (e.g., Datry et al. 2004). Punctual water sampling could complement this set-up in order to analyse major ion and trace pollutant species. The inherent sparsity of monitoring points raises the question of the representativity of the generated data and of the generalization of the observed trend to the whole MAR system. The implementation of numerical model of flow and transport describing the continuum between the vadose zone and the aquifer may provide a more general view of the fate of the infiltrated water and associated contaminants.

In general, groundwater flow and contaminant transport models are used to determine a variety of parameters such as: the velocity of groundwater and their piezometric levels, the fate of contaminants and their concentrations in the groundwater and the aquifer response to recharge (Merritt, 1985; Merritt, 1986; Brown, 2005; Maliva et al., 2006). The most commonly used models for simulating flow in groundwater are based on the Darcy's law (Darcy, 1856) for the saturated zone (or aquifer) and its extensions to unsaturated flow conditions based on Richards equation (Richards, 1931). The non-reactive transport models for solute are based on the Advection Dispersion Equation (ADE) (Eusuff and Lansey, 2004, Tutulic et al., 2011, Rahman et al., 2013, Winiarski et al., 2013). This model could be extended to include geochemical and biogeochemical reactions (e.g., Tzoraki et al., 2018). Over the last decade, few studies evaluated the potential of such models to simulate artificial groundwater recharge and associated transport of contaminants. A groundwater model with transport and particle tracking was employed by Eusuff and Lansey (2004) in order to find the best management model for the recharge operation of aquifer taking into account the water quality changes. This model based on Darcy's law was applied on two examples of a general hypothetical aquifer (the domain of aquifer is bidimensional) and the infiltration rate was assumed to be constant. In another case study (Rahman et al. 2013), Darcy's law combined with other techniques (spatial multi-criteria decision analysis) was used to investigate the most suitable site for the implementation of managed aquifer recharge. Their model is based on simplified 2D geometries with a constant infiltration rate. Tutulic et al. (2011) developed a 3D numerical model in order to explore the risks associated with aquifer recharge using storm water. This model combines both saturated and unsaturated zones of aquifer by using the Richards equations. The domain of the adopted model was determined from the topography of the field but recharge estimation was based on simplified water-balance model and did not take into account the variations of the water inflow over the time. A similar model to Tutulic et al. (2011) was employed by Tzoraki et al. (2018) for the assessment of the operation efficiency of a MAR system in Cyprus. In this study, the model was coupled with the geochemical model PHREEQC in order to take into account the chemical composition of water mixing with reactive contaminants (i.e., phosphate and copper). Their work combine laboratory analyses with hydrogeological and geochemical modelling. It was based on a simplified geometry because the real topography of the river-aquifer system (shape of the water table surface, geometry of the river, river-aquifer exchange limit) was not implemented. After analysis of these previous works, the main observation was that the modelling of groundwater recharge from infiltration basins in 3D configuration remains poorly studied and are rarely based on time series measurements to estimate water recharge. Consequently, model outputs could be only roughly compared with field measurements.

To circumvent this problem, the present study of 3D numerical modelling was based on the well instrumented MAR site of Django Reinhardt in Chassieu (Lyon Metropole, France). Field measurements were obtained in the framework of the French field observatory for urban hydrology (OTHU). Previous works (Chastanet et al., 2008; Foulquier, 2010) already proposed numerical models of this site. These models were based on Darcy and Richards equations coupled with convection-dispersion equation for heat transfers. They simulated the effect of infiltration basin on piezometric levels and temperature. However, these studies were carried out in 2D and did not take into account the real geometry of the basin. Indeed, only two monitoring piezometers were used for calibration. The recharge estimation was generally underestimated.

In this paper, a 3D groundwater flow and solute transport model was built considering both the unsaturated zone and the aquifer by solving the Richards equation and the Advection Dispersion Equation (ADE). The operation of infiltration basins in terms of water and solutes transfers were simulated in a realistic 3D geometry based on topographic data. In a first step, the flow model was calibrated against distributed piezometric data. The transport properties were calibrated against electrical conductivity data. Finally, the fate of a tracer solute was simulated during rainfall event. The ultimate goal of this work is to provide a representative distribution of the flow and solute tracer in the MAR system. An analysis of the 3D flow field and of the dynamics of the injected solute mixing in the aquifer is proposed. These results can be of prime interest to interpret biochemical measurements carried out classically in piezometers located around the basin.

II- Materials and Methods

The experimental site named Django Reinhard basin (DjR) is located in Chassieu in the eastern suburbs of Lyon, France (Fig.1). It is instrumented and monitored in the framework of French field observatory for urban hydrology (OTHU in French: http://www.graie.org/othu/)). The storm water catchment of Chassieu was selected as being representative of an industrial catchment found in developed countries. The total surface is 185 ha, with a flat topography (mean slope of 0.4%) and an impervious ratio of about 75% (Barraud et al., 2002; Bertrand-Krajewski et al., 2004). The catchment is drained by a separated storm sewer system. It also receives dry weather effluent (clean cooling water from industrial processes). Its outlet is the DjR basin which is composed of two compartments connected with a 60 cm diameter pipe: (i) a detention and settling basin and (ii) an infiltration basin, each of about 1 ha. The corresponding volumes to the two basins are 32000 m^3 and 61000 m^3 respectively.

The Django Reinhard infiltration basin is located over quaternary fluvial and glacial deposits of the St Laurent de Mure-Decines-Chassieu corridor (oriented SE-NW) according to the work of Barraud et al. (2002), Bertrand-Krajewski et al. (2004) and Goutaland et al. (2008). The thickness of the deposits in this corridor is approximately 30 to 35 m and the aquifer is located approximately 13 m (average water table) below the bottom of the infiltration basin (Barraud et al., 2002; Bertrand-Krajewski et al., 2004). The aquifer has a mean hydraulic conductivity of 7 to 9×10^{-3} m. s^{-1} (BURGEAP, 1995). According to grain size analyses, the sediment is quite homogeneous at the metric scale, promoting a high degree of homogeneity of the aquifer (Barraud et al., 2002; Bertrand-Krajewski et al., 2004).

A groundwater monitoring and data acquisition system was set up in order to evaluate the infiltration hydrological regime and the seasonal variations of the contaminants transiting into the aquifer. It also includes flow and pollutant loads measurements at the Django Reinhardt basin inlet. This monitoring system provides detailed information about the impact of recharge on groundwater quality. On the Django Reinhardt site, the water level in the basin is measured continuously (two minutes' time-step) by four piezoresistive sensors placed at different points of the basin. The quality of the water entering in the infiltration basin is continuously evaluated (2 minutes' time-step) by measurements of turbidity, pH, electrical conductivity and temperature. These measurements are carried out in a bypass channel receiving water pumped out of the main inlet pipe. Groundwater level, electrical conductivity and groundwater temperature are measured continuously (every hour) using multi-parameter LTC Levelogger® Junior probes (Solinst, Canada). These probes are installed in control piezometers (SC1, SC7, SC12, SC13 and SC29) located around the basin (Fig. 1). The depths of the sampling points are: 183 mNGF for SC12, 182.2 mNGF for SC7, 182.5 mNGF for SC13, 184 mNGF for SC1 and 182.2 mNGF for SC29. All devices are working continuously and are connected to data loggers. More details about this experimental setup can be found in Barraud et al. (2002).

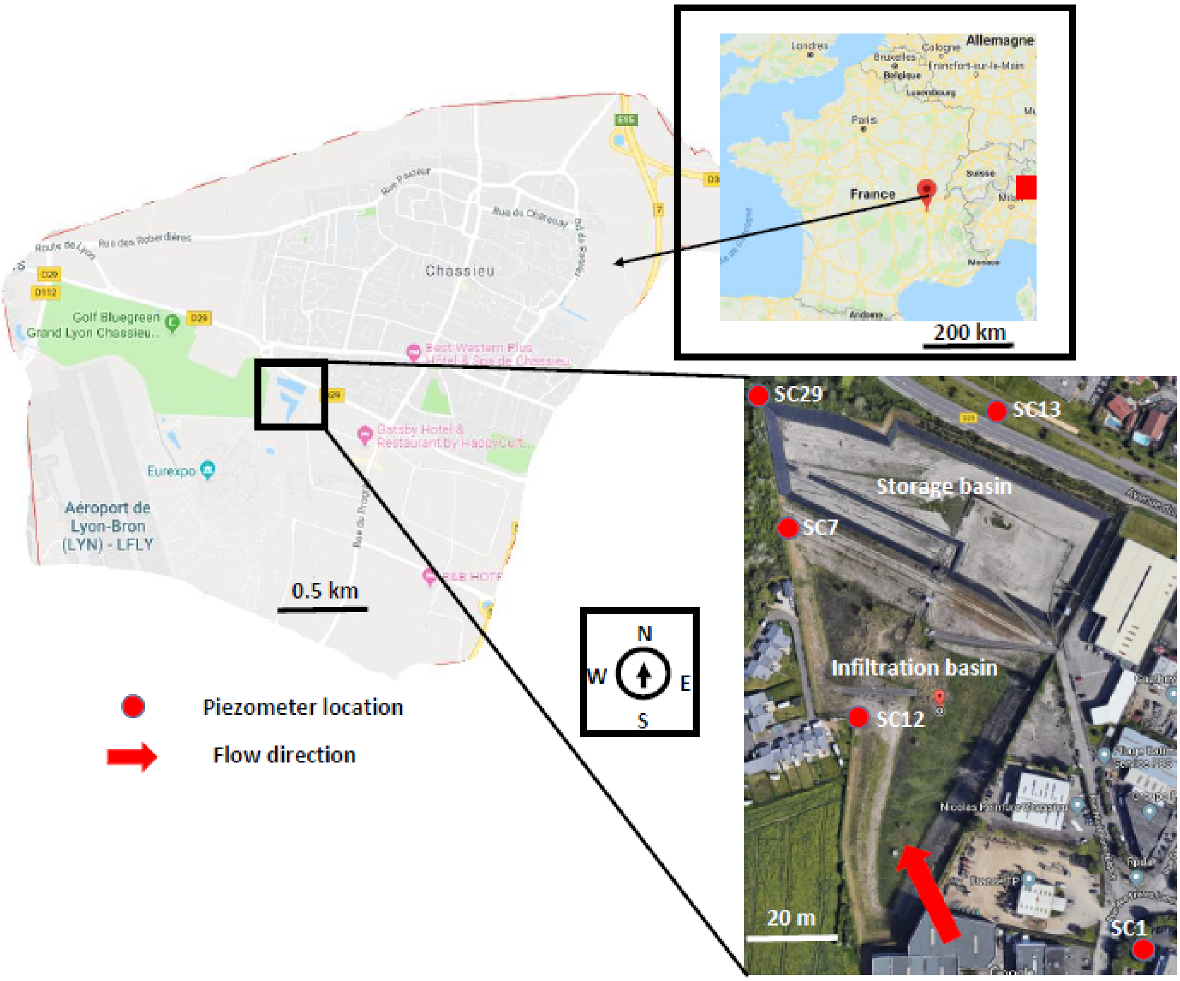

Fig.1. Study site location and aerial view of the Django Reinhardt basin. Data source: Pictures and Maps are from Google Maps

III- Development of the 3D managed aquifer recharge model

The development of the 3D model of the Django Reinhardt experimental site was carried out in several stages. The first step consisted in building the geometry of the model from actual field data. Then, a numerical model was carefully chosen to simulate the flow and transport of solutes in both the saturated and unsaturated zone of the fluvio-glacial aquifer below the infiltration basin. The calibration strategy was based on trial-and-error: in a first step, the finite element tetrahedral mesh was optimized. A refinement was applied to the vadose zone and the top of the aquifer beneath the basin to improve the numerical convergence of the non-linear iterative resolution of Richards equation. In a second step, the hydrodynamics parameters were adjusted to match field data. Then, the model is able to carry out a sensitivity study of the parameters controlling the impact of the infiltration basin and to test the model on other infiltration scenarios (contrasting volumes of infiltrated storm water, contrasting concentrations of pollutants drained to the basin).

Simulations were carried out with the finite element software Comsol Multiphysics 5.4, a general-purpose simulation software for modelling designs, devices, and processes in all fields of engineering. For theoretical and practical information regarding the model use and the solution of the flow and transport equations, the reader may refer to the software manual (see the bibliography). It was chosen for this study because it offers flexibility to simulate complex geometries and to refine the mesh around areas of interest (observation points, basin-aquifer exchange limit, etc.). In addition, it includes a user friendly graphical interfaces for model building, model input and post-processing of model output.

III-1 Model geometry

The model was built in order to reproduce the main characteristics of the Django Reinhardt experimental site. The geometry of the basin was constructed from a digital elevation model obtained from the IGN (French National Geographic Institute). The resolution of the digital elevation model (DEM) is 1 m as shown in Fig. 2.

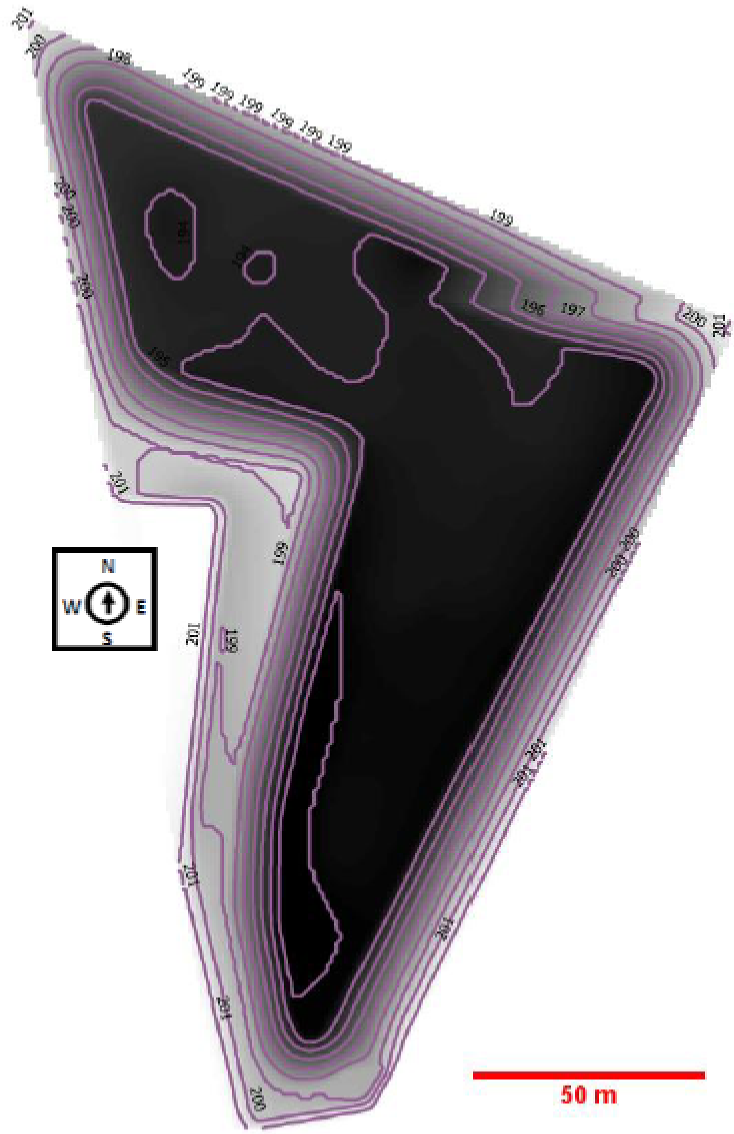

Fig.2. Topography of the Django Reinhardt infiltration basin: French projected coordinate system RGF93/Lambert 93 (in meter)

The geometric construction of the model was done in two steps. The first step was the construction of the aquifer domain. The aquifer is materialized by a 3D rectangular domain (1000m * 600m * 30m) covering the whole study area. This domain is oriented to match the aquifer main flow direction. Then, the infiltration basin is imported into the 3D aquifer domain. The treatment of the basin DEM was carried out using the QGIS software. This construction respects the geo-referencing of the piezometers used as observation points. The final form of the DjR basin coupled with the aquifer domain is shown in Fig.3. The three-dimensional finite element mesh was generated after the building of the geometry. The mesh is refined in the infiltration zones. The mesh is constituted of 26142 triangular elements on surfaces and 181586 tetrahedral elements in volume. The final shape of the meshed computational domain is illustrated in Fig.3.

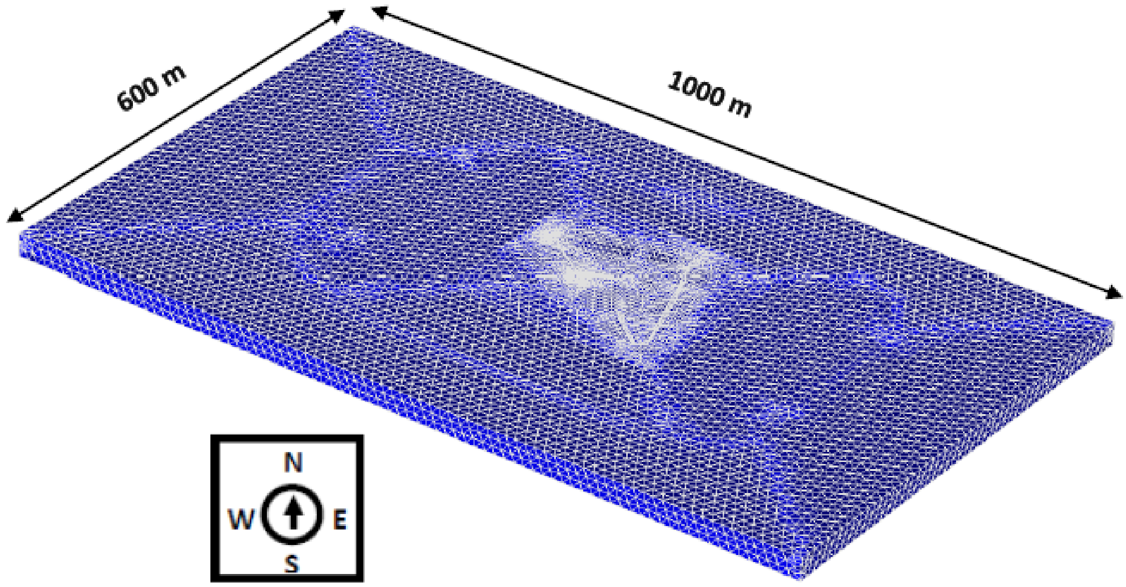

Fig.3. Three dimensional model of the Django Reinhardt (DjR) experimental site

III.2 Description of numerical model

The unsaturated water flow in the study site is described using the well-known Richards equation (Richards, 1931) with no sink term (Eq. (1)):

$$\frac{\partial \theta}{\partial t} = -\nabla.(K_s kr(\theta)(\nabla h + 1)) \qquad (1)$$

where θ ($m^3.m^{-3}$) is the volumetric moisture content, t (s) the time, K_s ($m.s^{-1}$) the saturated hydraulic conductivity tensor, kr (-) the relative permeability and h (m) the suction. Due to the sedimentary nature of the soil, the hydraulic conductivity tensor K_s is considered diagonal with vertical and horizontal components (K_{sv} and K_{sh} respectively).

The moisture content could be conveniently expressed as the effective saturation S_e:

$$S_e = \frac{\theta - \theta_r}{\theta_{sat} - \theta_r} \qquad (2)$$

where θ_r ($m^3.m^{-3}$) is the residual volumetric moisture content and θ_{sat} ($m^3.m^{-3}$) is the saturated volumetric moisture content (or the active porosity).

The numerical resolution of Eq. (1) requires the knowledge of the water retention curve ($S_e(h)$) and the relative permeability curve (θ (h)). It is modelled by the classical Van Genuchten-Mualem equations (Van Genuchten, 1980; Mualem, 1976):

$$S_e(h) = \left(1 + (\alpha|h|)^{1/(1-m)}\right)^{-m} \qquad (3)$$

where α (m^{-1}) and m are Van Genuchten fitting parameters

$$k_r(h) = \sqrt{S_e}\left(1 - \left(1 + (\alpha|h|)^{1/(1-m)}\right)^{-m}\right)^2 \quad (4)$$

Van Genuchten parameters (α and m) and the saturated and residual moisture contents (θ_r and θ_{sat}) are classically estimated from laboratory measurements. In the present study, these parameters are directly calibrated against field data during a real rainy event in order to depict the large scale heterogeneity of soil properties.

The transfer of dissolved solutes in soils is often modelled by the advection-dispersion equation (ADE). For unsaturated soils, it reads:

$$\frac{\partial \theta c}{\partial t} + \mathbf{u}.\nabla c = \nabla.(\theta D_{eff} \nabla c) \quad (5)$$

where c is the liquid molar concentration ($mol.m^{-3}$), u is the velocity field ($m.s^{-1}$) and D_{eff} is the dispersion tensor ($m.s^{-2}$).

The coupling between equations (1) and (5) due to the volumetric moisture content θ generated convergence problems in the numerical solution. In order to overcome this difficulty, θ was set constant in the vadose zone ($\theta = \theta_e$).

The velocity field **u** is derived from equation (1) as the generalized Darcy law:

$$\boldsymbol{u} = - K_s k_r(\theta)(\nabla h + 1) \quad (6)$$

The components of dispersion tensor, i.e., the longitudinal D_L and transversal D_T dispersion coefficients can be expressed as (Bear, 1972):

$$D_L = \alpha_L \frac{|u|}{\theta} + \tau D_0 \quad (7)$$

$$D_T = \alpha_T \frac{|u|}{\theta} + \tau D_0 \quad (8)$$

where α_L (m) and α_T (m) are the medium longitudinal and transversal dispersivities, τ (-) is the medium tortuosity set to $\theta^{-1/3}$following Millington and Quirk (1961) and D_0 ($m.s^{-2}$) is the solute molecular diffusion coefficient.

In order to represent the concentration measurement based of punctual integrative samplers located in piezometers used in studies of emerging contaminants of concern, the averaged concentration C_m ($mol.m^{-3}$) is calculated as:

$$C_m = \frac{1}{T}\int_0^T c\,dt \quad (9)$$

where T is the time of exposure fixed at 10 days in this study.

III.3 Initial and boundary conditions of the model

In order to solve the mathematical model (Eq. (1) to (8)), initial and boundary conditions (IC and BC respectively) are required for the flow and solute transfer models. Conditions for the flow model were defined as follow:

- A linear hydraulic head $H_0(x,y)$ is interpolated between the inlet and outlet boundaries of the aquifer in order to impose the average water table level observed as IC. The suction in the vadose zone is then forced to be hydrostatic.
- During the simulation, constant hydraulic heads are set at the inlet and outlet BC of the aquifer. These limits match the hydraulic gradient set as initial conditions.
- For the infiltration fluxes (in $m.s^{-1}$), the BC set in the basin is a time series calculated from the basin water mass balance. It is equal to zero when the basin is empty.
- All the other BC (at the bottom, top and lateral faces of the domain) are set as no flow BC.

Two types of IC and BC are used for the solute transfer equation (Eq. (5)). In a first step, the concentration is used to represent electrical conductivity dynamics. This approach is questionable due to the numerous factors influencing water electrical conductivity (such as temperature and concentrations of all ionic species with various mobility and sorption behaviour). However, it has the benefit to set a constraint on the transport effective properties (θ_e, α_L and α_T) based on field monitoring data. As storm water is lowly mineralized (with a low electrical conductivity) in comparison with groundwater, we assume that electric conductivity of water was a pertinent marker to follow the storm water plume in groundwater (e.g., Datry et al. 2004, Voisin et al. 2018). In a second step, an adimensional concentration is considered to simulate the behaviour of a generic solute tracer.

- The electrical conductivity IC is imposed to 650 μS/cm in the aquifer to match the average value measured before the studied rain event. This value is also imposed in the unsaturated zone since no data are available concerning the electrical conductivity of the water trapped by capillarity at the initial state. For the generic solute tracer, the initial conductivity is null.
- The IC value is imposed as BC at the aquifer inlet.
- The aquifer outlet BC is of type free flow corresponding to a pure advective BC (i.e. no diffusive flux).
- For the BC of the model in the infiltration basin, a fixed water electrical conductivity is imposed when the water infiltrates. For the electrical conductivity simulations, this value is evolving with time following the time series of measurement at the basin inlet. For the generic solute tracer, the injected concentration is set to one ($c = 1$). This BC switches to a no flux BC when the basin is empty.

- All the other BC (at the bottom, top and lateral faces of the domain) are set to no flux BC.

III.4 Computation of the infiltration flux

The evaluation of aquifer recharge via the infiltration basin was made by considering an imposed flow condition. The infiltration flux is calculated through a water mass balance in the basin. Infiltration occurs only through the bottom of the basin, with dikes considered impermeable in this calculation. The mass balance is based on the flowrate measurements at the basin inlet expressed as:

$$\frac{V(t)}{dt} = Q_e(t) - Q_{inf}(t) \qquad (10)$$

where V (m^3) is the volume of water in the basin (m^3) at time t (s), Q_e ($m^3.s^{-1}$) is the measured water flow at the basin inlet and Q_{inf} ($m^3.s^{-1}$) the infiltrated water flow.

The volume of water in the basin is calculated from the water level measurements carried out in the basin using the topographic data obtained via the DEM. Considering that the basin has a constant area A_b (m^2), the Eq. (10) is written as:

$$A_b\frac{dH_b(t)}{dt} = Q_e(t) - Q_{inf}(t) \qquad (11)$$

where H_b (m) is the measured water level in the basin.

The Eq. (11) is integrated numerically using a Matlab code in order to estimate the evolution of the infiltration flux with time. This calculation integrates the entire history of flowrate and water level in the basin for the period or rain event under consideration. Finally, the infiltration function obtained is imposed as BC in the 3D model.

IV- Results and discussion

IV-1 Calibration of the 3D groundwater flow model: Comparison of piezometric levels between observed and simulated observation points

The calibration of the 3D groundwater flow model is based on the simulation of the infiltration of water during a rain event. This rainy episode from January 3rd to 6th in 2018 was chosen from the data measured by the OTHU at the Django Reinhardt site. The choice of this particular rainy event was made due to its high intensity and duration. It was an individual event not disturbed by other rainfall events that could affect the aquifer response. The Fig. 4 presents this rainy episode (precipitation over time) and the corresponding flowrate measured at the basin inlet. It is worth noticing that the basin catchment presented a quick response to the rain with a maximum infiltration flow rate reached before the rainfall intensity pick. The infiltration flow rate exhibited a strong decrease at the end of the even corresponding to the beginning of a progressive emptying of the basin that lasted approximately 18h after the end of the rain fall.

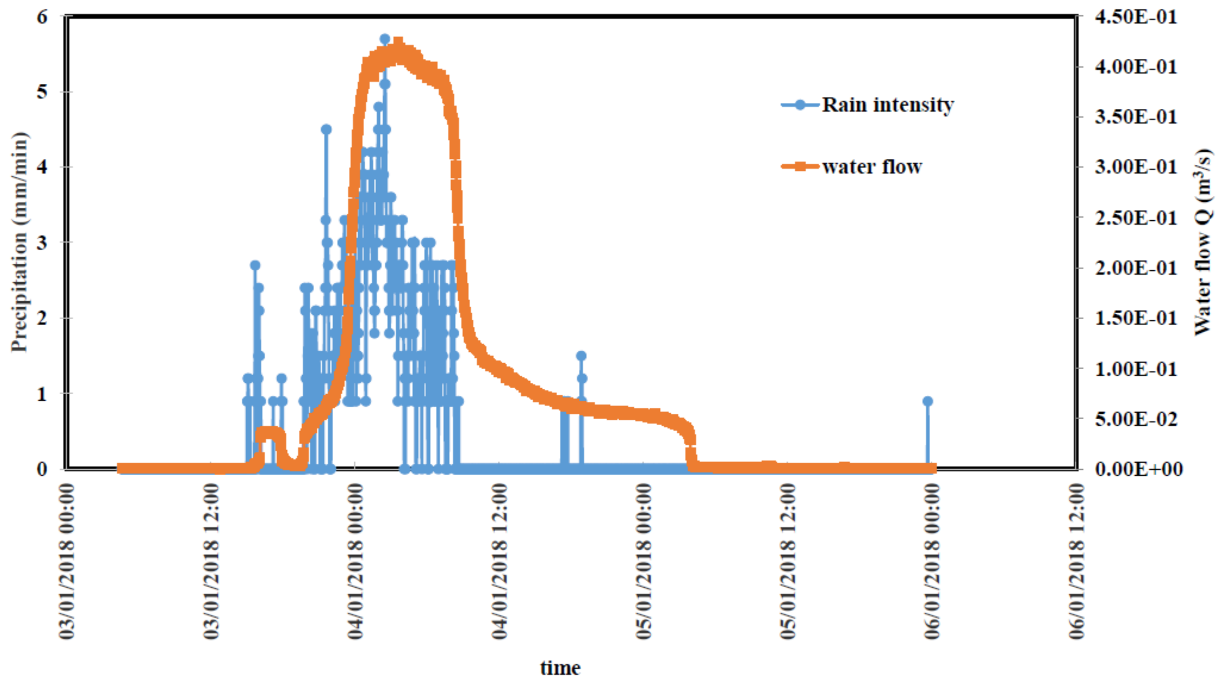

Fig.4. Rain intensity and water fluxes at the basin inlet during the rainy episode from January 3 to January 6, 2018.

A trial-and-error approach was used to estimate the flow parameters in order to reproduce the piezometric response of the aquifer around the basin. These simulations are carried out over 7 days: 1.8 days for the rainy episode and 4.2 days to observe the relaxation of the system after the rain. The computation time step is limited to 0.005 days in order to limit the numerical oscillations. The flow parameters to be calibrated are the porosity (θ_{sat}), the residual saturation in water (θ_r), the vertical and horizontal permeability (K_{sv} and K_{sh} respectively) as well as the parameters of the Van Genuchten equation (α and m). These parameters are adjusted so that the response of the aquifer in terms of groundwater levels corresponds to field observations. The Fig. 5 shows the comparison of simulated and observed groundwater levels on 5 piezometers (see location on Fig.1).

The piezometer SC12 exhibited the stronger response with an observed increase of the water table level of about 0.9 m due to its location in the close vicinity of the basin in the L-shape corner. Even if the model captured adequately the dynamic behavior, it slightly underestimated the water table level increase with 0.7 m at the maximum. Piezometers SC7 and SC29, located in the downstream direction of the aquifer, presented a similar agreement with the monitoring data with an underestimation of the maximum level lower than 0.1 m compared to their respective maximum increase of 0.4 m and 0.35 m respectively. The model resulted in a slight overestimation of the water table increase on the lateral piezometer SC13. Finally, the piezometer SC1 located about 50 m upstream the basin exhibited a lower increase compared to the monitoring data. Modelling results globally show an acceptable restitution of the measured data considering the complexity of the real system, i.e., the spatial heterogeneity of the entry conditions in the basin (distribution of water level in the basin for example) and the spatial heterogeneities of the hydrodynamic properties of the unsaturated zone (these parameters are considered to be constant in the model).

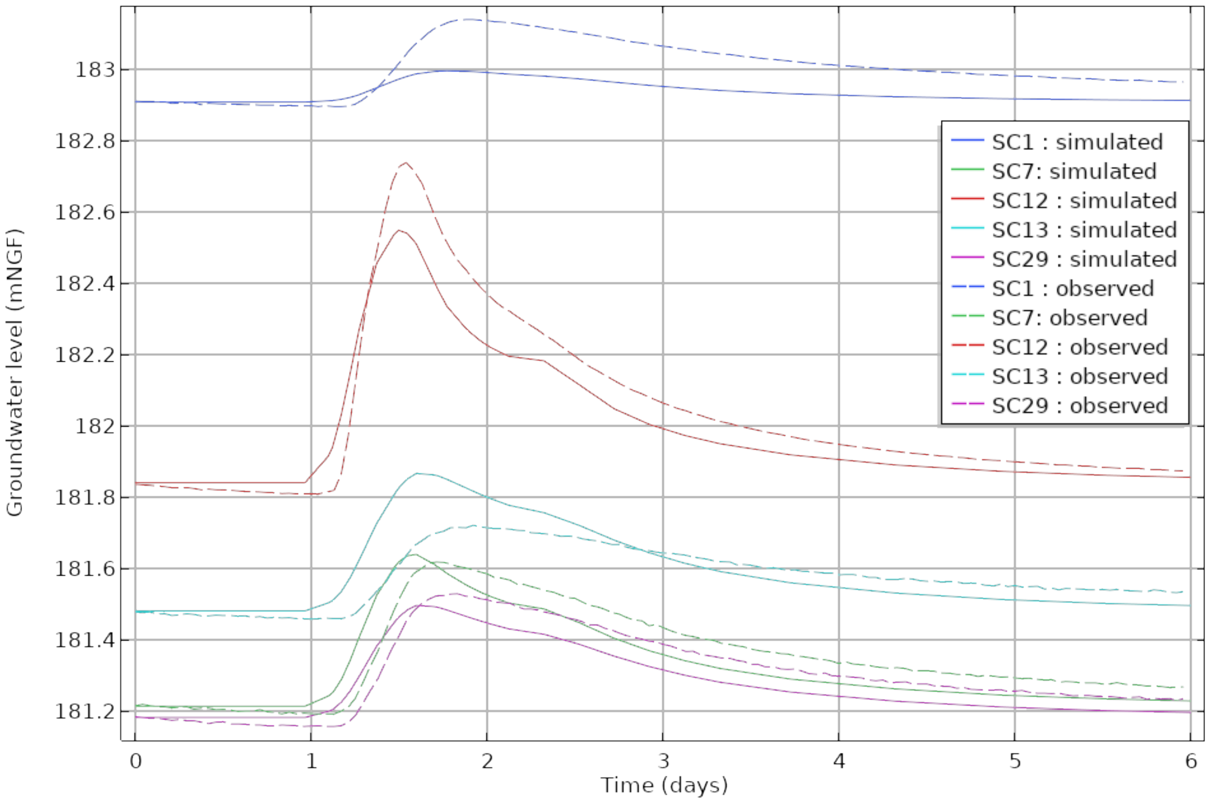

Fig.5. Comparison of piezometric levels between observed and simulated observation points during the rainy episode from January 3 to January 6, 2018.

The parameters obtained after the model calibration are presented in Table 1. The calibration step particularly highlighted the need to consider a low value of active porosity ($\theta_{sat} - \theta_r = 0.12$). This result is coherent with the assumption of a dual permeability medium proposed by Winiarski et al (2012). In our model, the flow only occurs in the soil macro-porosity (as observed by Slimene et al. 2017 in unsaturated zone of the studied basin). The hydraulic conductivity of order of magnitude around 10^{-4} m/s is also coherent with the fluvial/glacial origin of the sedimentary deposits. The anisotropy ratio of around 8 between the horizontal and vertical permeability corresponds well to the stratified nature of these deposits. This is worth to note that an anisotropy ratio of about 100 was necessary to fit the results with a 2D model in Foulquier et al. (2010). This difference put forward one of the benefice of 3D simulations which distribute the flow all around the basin in a more realistic manner.

Table 1: Values of the flow parameters retained after the calibration procedure of the model

Flow parameters	**Retained value**	**Unit**
Porosity θ_{sat}	0.13	m^3. m^{-3}
Horizontal permeability K_h	6.00 10^{-3}	m.s^{-1}
Vertical permeability K_v	8.00 10^{-4}	m.s^{-1}
Residual moisture content θ_r	0.0065	m^3. m^{-3}
Van Genuchten parameters α	1	m^{-1}
Van Genuchten parameters m	0.5	-

A sensitivity study on the influence of permeability on piezometric level was performed during the model calibration. The effect of horizontal and vertical permeability is presented in Fig. 6. This result highlights the strong effect of the horizontal permeability on the aquifer response. The piezometric level increases by a factor 2 if the horizontal permeability is reduced by a factor of 5 corresponding to an almost vertical flow in the vadose zone. A similar decrease of the vertical permeability promotes a spreading of the flow resulting in a smaller response of the aquifer.

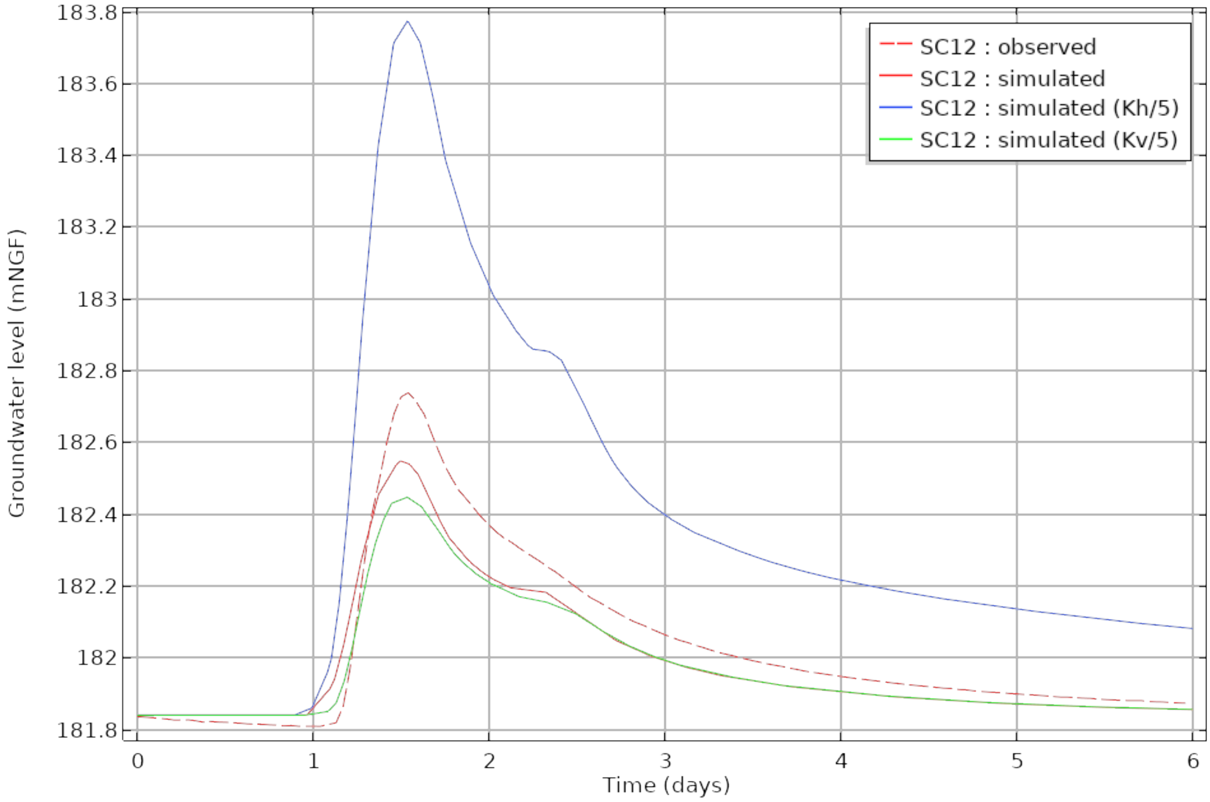

Fig.6. Influence of permeability on the piezometric levels (rainy episode from January 3 to January 6, 2018).

In order to have a more spatialized view of the flow during the infiltration-drainage processes, it is convenient to plot the current lines coming from the basin and the aquifer inlet (Fig.7). At the initial state (0 days) (Fig.7a), the recharge due to the basin is null. The level of the water table is not influenced by the basin and the flow is horizontal in the aquifer. At the maximum of recharge (1.5 days) (Fig.7b), the basin strongly affects the flow in the aquifer. The 3D image shows that the distribution of current lines coming from the basin is driven by the geometric shape of the basin. A significant lateral extension of these flow lines explains the significant piezometric response observed on the lateral piezometer SC13 theoretically located outside of the storm water plume in groundwater (Fig. 5). After the end of the infiltration (2.5 days) (Fig. 7c), a shrinkage of the current lines is observed which is characteristic of the drainage period. The flow below the basin gradually decreases until reaching before stopping after several days (6 days for the considered rain event).

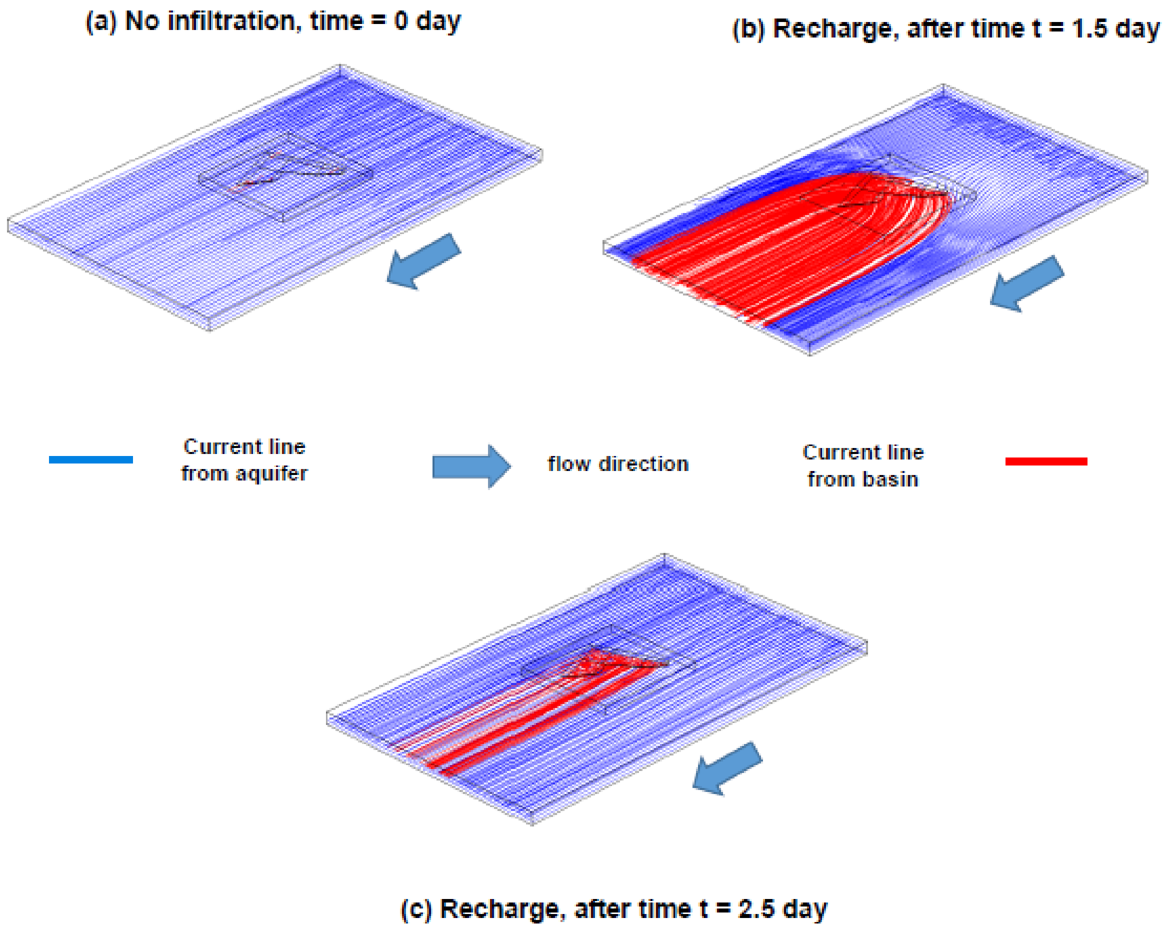

Fig.7. The current lines during the simulation of the reference rainy episode (image (a) corresponding to zero recharge, image (b) to 1.5-day period of recharge and image (c) to 2.5-day period of recharge).

In order to test the calibration on a longer scale, the model was used to simulate the MAR system during the month of December 2018. During this month, two major rain events followed by drainage periods including small rains were observed. The simulation result (Fig.8) shows an acceptable restitution of the variations of the piezometric levels recorded at the piezometers of control during the simulated period. The calibration carried out on January 2018 data allows describing the MAR system on December 2018. As a conclusion, the 3D model of the Django Reinhardt site implemented reproduces well the level of the groundwater on both a single event and a monthly time-series.

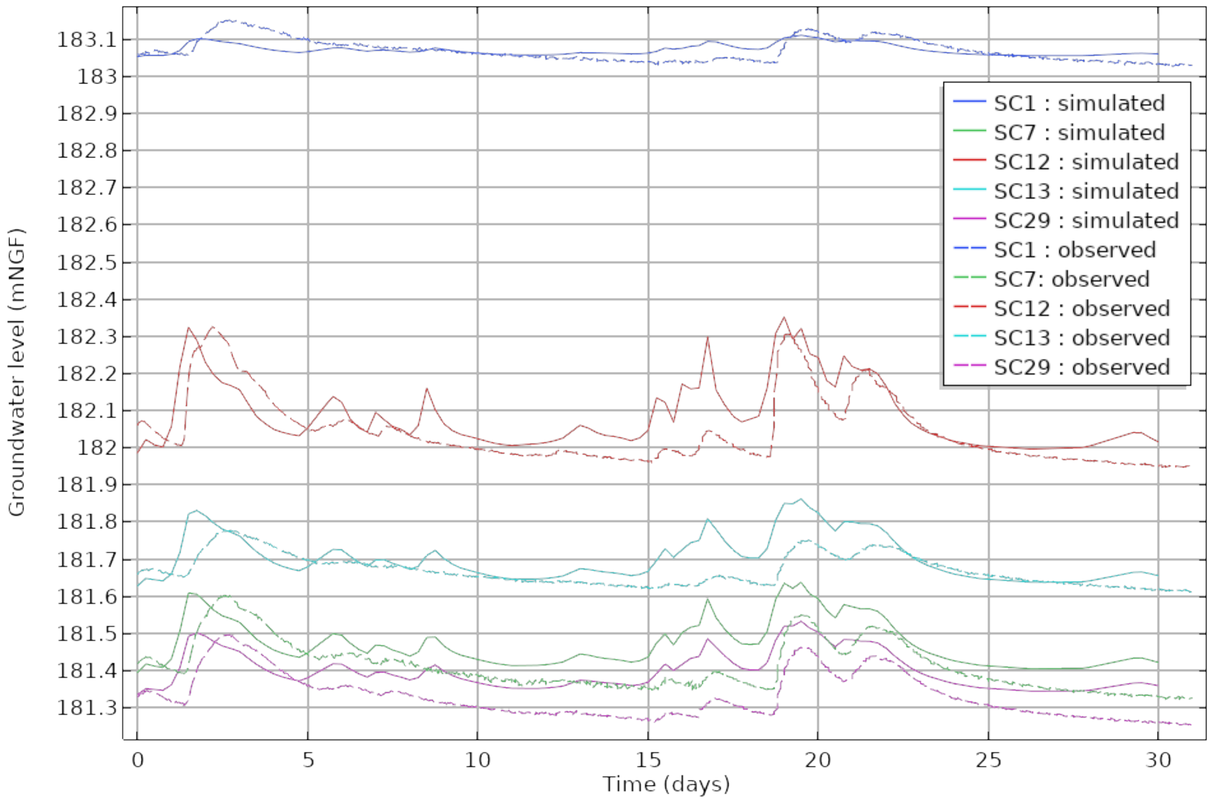

Fig.8. Comparison of piezometric levels between observed and simulated observation points during the month of December 2018

IV-2 Calibration of the 3D solute transport model: comparison of electrical conductivity between observed and simulated values

The transport model was calibrated like the groundwater flow model. For the calibration, the same rainy episode was considered and the simulations were carried out over 7 days: 1.8 days for the rainy episode and the following period to observe the relaxation of the system after the rain. Electrical conductivity was chosen as the reference parameter because of the availability of in-situ measurements. The values of electrical conductivity considered are the variations of electrical conductivity compared to initial values. This representation was chosen because the measured initial values at the observation points (piezometers) presented spatial heterogeneities while a homogeneous initial value was applied in the model. The parameters of the transport model to be calibrated are the effective porosity (θ_e), the longitudinal dispersivity (α_L) and the transversal dispersivity (α_T). An analysis of the results (Fig.9) shows that the simulation reproduces fairly well the electrical conductivity measured at the control piezometers placed around the basin even if the observed variations are low (10 to 15 µS/cm). The responses of piezometers SC7 and SC13 are properly modelled for the dynamics and the maximum decrease of electrical conductivity. The small decrease of electrical conductivity observed in the piezometer SC13 is not reproduced by the model. It is interesting to notice that this lateral piezometer exhibited a significant increase of the groundwater table level but appeared to receive a very small amount of solute.

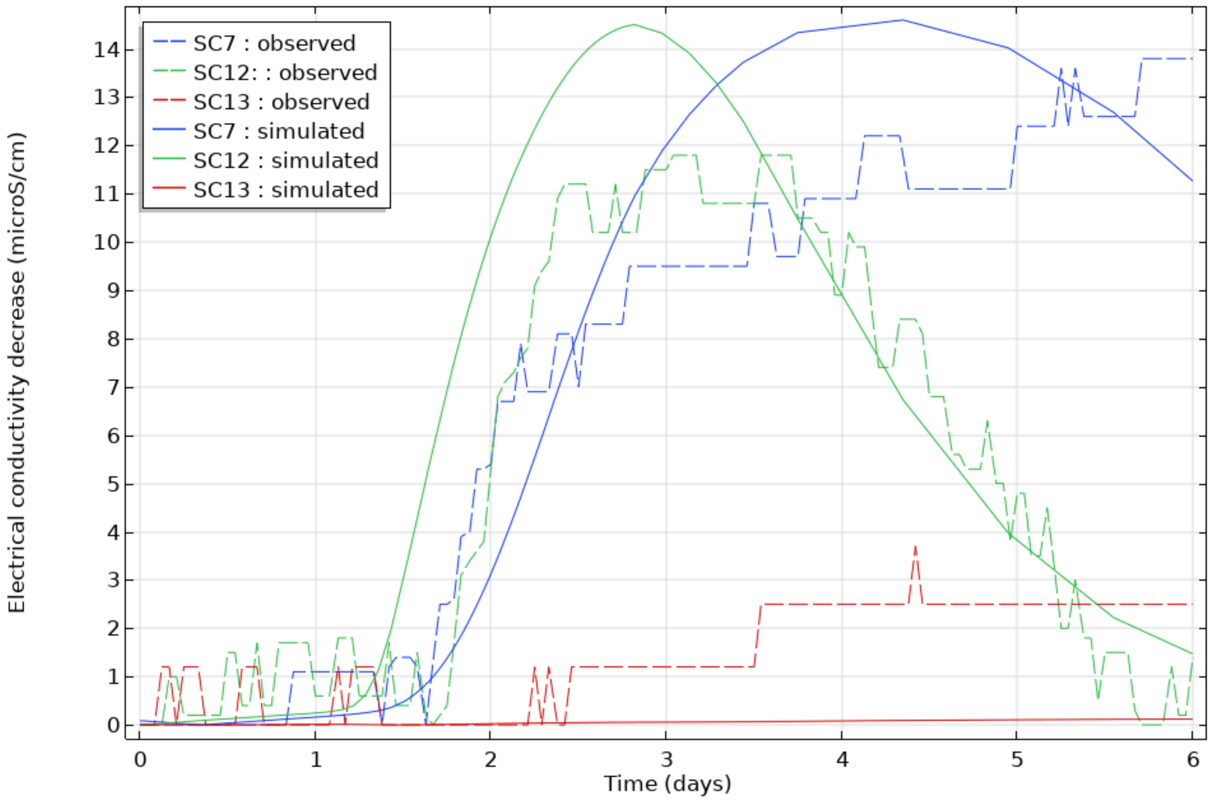

Fig.9. Comparison of electrical conductivity decrease between observed and simulated observation points during the rainy episode from January 3 to January 6, 2018.

The parameters selected after the calibration procedure are presented in Table 2. The effective porosity θ_e is in good agreement with the average water content observed in the vadose zone during the water infiltration. The molecular diffusion D_0 was set to a constant value representative of most dissolved species and was not adjusted during the calibration. The longitudinal α_L, with 2 m, has a value of between 1/5 and 1/10 compared to the thickness of the vadose zone. The transversal dispersivity α_T was classically set to 1/10 of the longitudinal dispersivity provided a reasonable response for piezometers SC7 and SC12. It was not possible to generate a noticeable response on the lateral piezometer SC13 by increasing α_T.

Table 2: Parameters values of the transport model retained after the calibration

Parameters of transport model	Retained value	Unit
Effective porosity θ_e	0.07	$m^3. m^{-3}$
Solute molecular diffusion coefficient D_0	$1.00\ 10^{-9}$	$m^2.s^{-1}$
Longitudinal dispersivity α_L	2	m
Transversal dispersivity α_T	0.2	m

IV.3 Simulation and analysis of the fate of a tracer infiltrated in the aquifer from the DjR basin

In this part, the fate of a pollutant considered as a tracer (most critical case) was simulated during the rainy episode of January 2018 presented previously. The 3D simulations of the tracer transport made it possible to highlight the effect of the observation points location on the representativeness of the chemical measurements made in the field. The previously calibrated transport model was used to perform these calculations. The simulation was carried out on 10 days after the beginning of the rain event to mimic passive integrative samplers that can be used in the field (e.g., Pinasseau et al. (2019) for passive integrative samplers of pesticide and pharmaceutic compounds).

IV.3.1 Evolution of the pollutant plume during the infiltration-drainage processes

The behaviour of a tracer assimilated to the pollutant was observed during the infiltration-drainage process. In Fig. 10, the evolution over time of the pollutant plume is represented by the isovalue surface for c = 0.2. It has been observed that the geometric shape of the basin has a significant influence on the dispersion of the pollutant plume. At the end of the water injection (Fig.10.a), the plume was mainly located in the vadose zone and just started mixing in the aquifer. After 5 days (Fig.10.b), the tracer spreaded in the aquifer while being advected downstream. After 10 days, the plume appeared thinning due to the progressive dilution with the clean water of the aquifer. A noticeable amount of tracer could be seen trapped in the vadose zone under the aquifer. A numerical volumetric integration of the concentration in the vadose zone showed that about 20% of the injected tracer never reached the aquifer during the simulation. This entrapment was mainly due to the intermittent functioning of the basin. As the basin emptied, the flow velocity in the vadose zone progressively diminished during the drainage phase. This process was characterized by a progressive decrease of the water content which reduced the soil relative permeability. After 10 days, the downward flow and the associated tracer transport almost stopped. Even if the exact amount of tracer trapped in the vadose zone by capillary phenomena is probably not estimated with accuracy by the model, several additional processes could even strengthen this phenomenon: sorption mechanisms are classically promoting a retardation of solute transport, and dual porosity mechanisms, supposed non-negligible in this site by Winiarski et al (2013), would also promote trapping due to the diffusion of solutes from the active porosity to the soil micro-porosity.

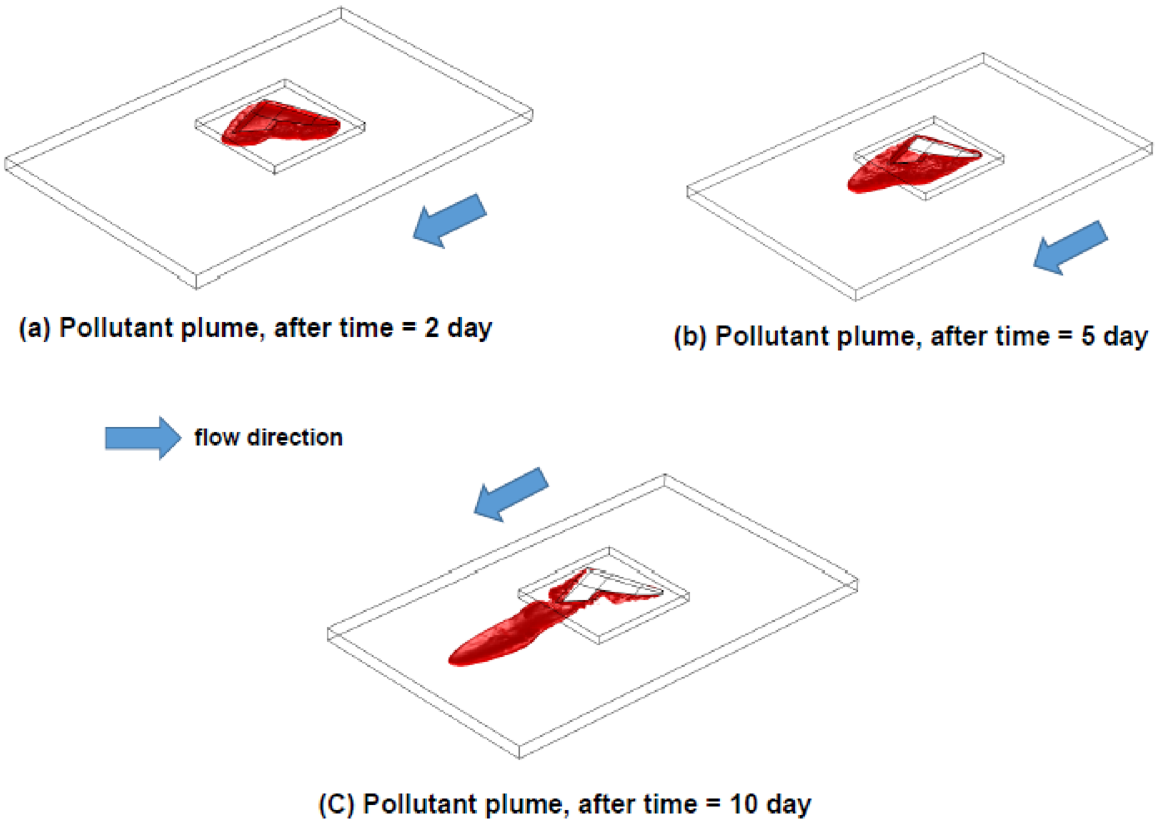

Fig.10. Evolution of the pollutant plume (isovalues at c = 0.2) during the infiltration-drainage process

IV.3.2 Implication on the use of passive integrative samplers: effect of piezometer locations on the estimate of pollutant concentrations

The effect of piezometers location on the estimate of pollutant fluxes was studied by using the post-treatment of the 3D calculation. The punctual time series of concentrations for some piezometers around Django Reinhardt site were analysed as 10-day average concentrations. This averaged concentration (C_m) varied between 0 and 25% of the injected concentration depending on the piezometer location (Fig.11). As previously observed on electrical conductivity results, the tracer plume does not reach the lateral piezometer SC13. The averaged concentration in piezometers SC7 and SC12 were very close with 25% and 24% respectively.

This result could appear trivial since both piezometers are located in the close vicinity of the basin in the downstream direction with similar sampling depth (183 mNGF and 182 mNGF in SC7 and SC12 respectively). However, it is worth noticing that the dynamics of tracer concentration exhibited very different behaviours. The response of piezometer SC12 was quicker with a high maximum concentration of 0.75. On the other hand, the piezometer SC7 only reached a maximum concentration of 0.53 but it was exposed to the tracer plume for a longer duration. This result provides an example of how purely hydrodynamic mechanisms tend to disperse solute species beneath the infiltration basin in a complex manner. This behaviour should be taken into account while analysing concentration measurements in the field. The use of punctual water sampling should be considered only with a high sampling frequency in order to avoid missing the contaminant migration at the piezometer. On the other hand, the use of passive integrative samplers could provide more robust data even if the analysis of resulting averaged concentration should be considered with care.

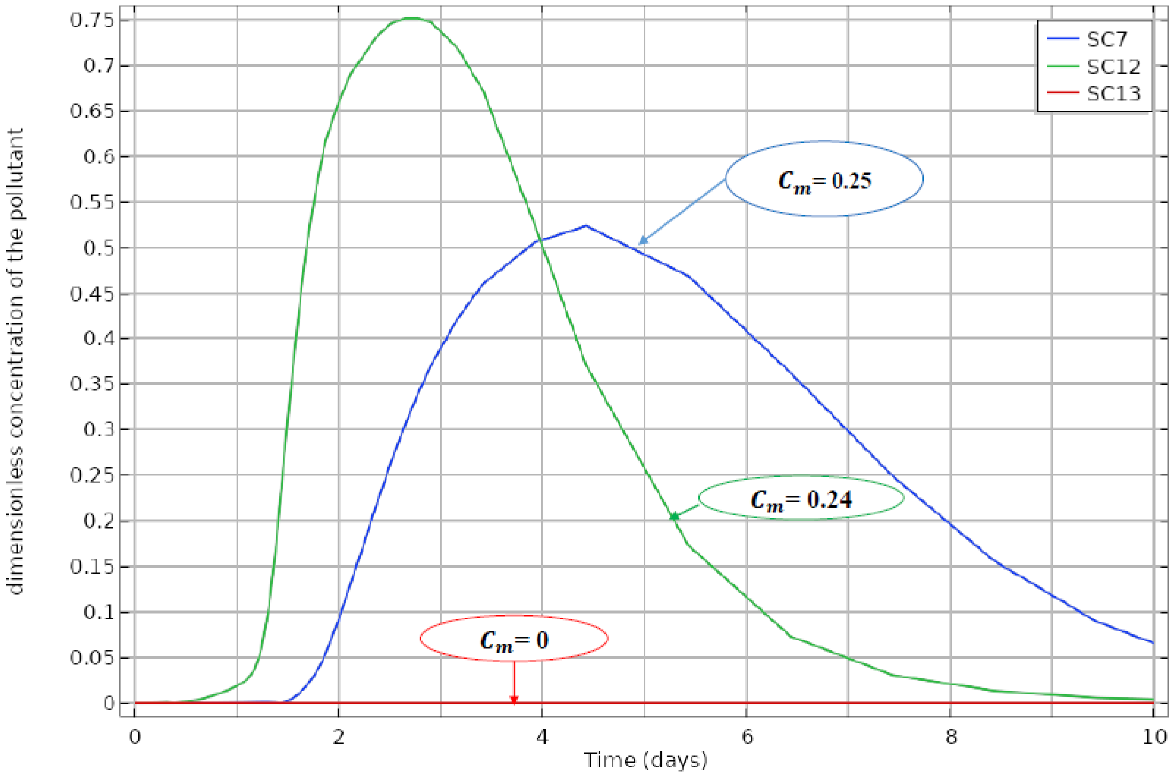

Fig.11. Effect of piezometers location on the estimate of pollutant fluxes

IV.3.3 Implication on the use of punctual integrative samplers: effect of integrative sampler depth on the estimate of pollutant concentrations

The piezometer SC12 located close to the basin was selected to highlight the effect of the depth of sampling points on the pollutant concentration estimated by passive integrative samplers (e.g., Pinasseau et al. 2019). Three virtual positions in this piezometer were considered: 1 m, 5 m and 10 m below the initial water table level (Fig.12). The evolution of the pollutant concentration (tracer) over time for the three depths of the integrative sampler is shown in Fig.12. The upper sampling point exhibited an average concentration of 0.3 which is 25% higher than the middle point. The lower sampling point resulted in a decrease of the average concentration down to 0.13 (approximately 50% lower than the middle point). This large differences are directly linked with the mixing of the infiltrated water in the upper part of the aquifer. This mixing behaviour should be kept in mind while analysing data from multi-parameter probes or chemical samplers specially if various sampling points with different depth are considered.

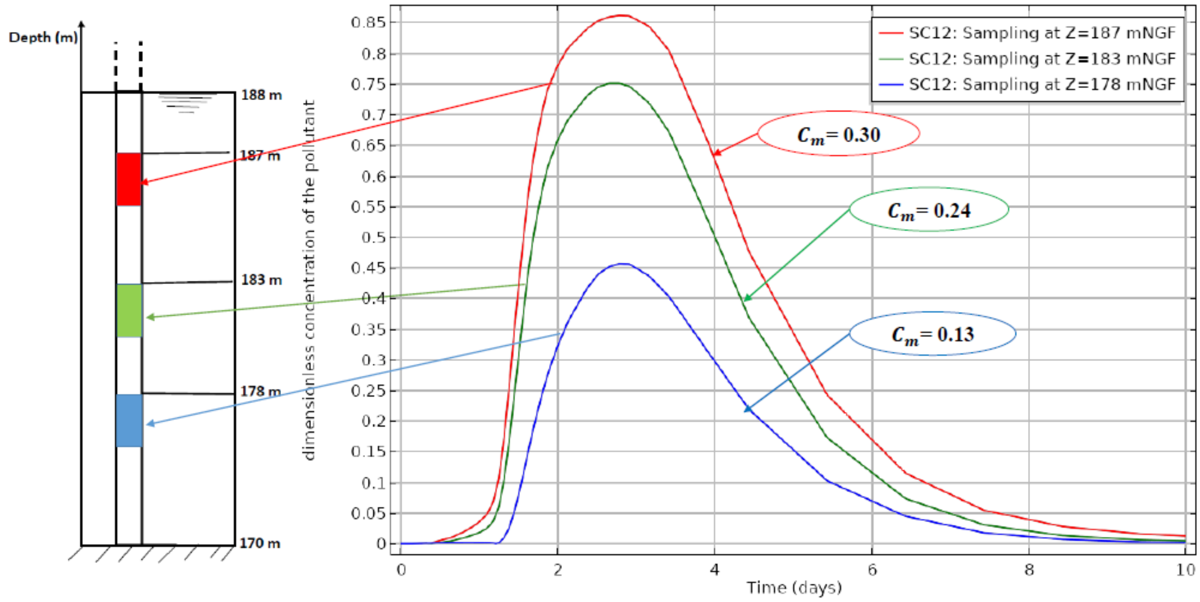

Fig.12. Effect of integrative sampler depth in the piezometer SC12 on the estimate of pollutant concentration

V-Conclusions

This study put forward the capability of 3D numerical model based on Richards equation and ADE to simulate adequately the impact of a storm water infiltration basin on its aquifer. It put forward the complex 3D shape of potential contaminant plumes and the subsequent precaution necessary to analyse chemical measurement carried out in piezometers. In the DjR basin site, the presence of a thick vadose zone beneath the basin provided a large volume of soil which promote capillary trapping of up to 20% of the tracer injected during a high intensity rainfall event. This stirage capability should be very beneficial to favour aerobic biodegradation of organic contaminants.

The 3D modelling approach is very promising to improve the evaluation of groundwater contamination by storm water infiltration. The modelled concentrations of pollutants (% of injected concentration in the basin) recovered from each piezometer depending on its location can be a very pertinent way to evaluate the environmental impact of basins on groundwater quality. This approach may be also pertinent to evaluate the retention processes occurring during the transport of contaminants from the basin to the aquifer. With this aim, experiments using integrative passive samplers to evaluate pollutant contents in the field would be required to compare observed and modelled concentrations of contaminants.

Acknowledgment:

This study was funded by the French National Research Agency (ANR FROG). It benefits from the support of the OTHU (Observatoire de Terrain en Hydrologie Urbaine, supported by Métropole de Lyon) which provides high resolution monitoring data concerning surface and groundwater.

References:

Barraud, S., Gibert, J., Winiarski, T., Bertrand-Krajewski, J.-L., 2002. Implementation of a monitoring system to measure impact of stormwater runoff infiltration. Water Sci. Technol. 45, 203-210.

Bates, B., Kundzewicz, Z.W., Wu, S., Palutikof, J., 2008. Climate Change and Water, pp. 1-214 (Geneva).

Bear J., 1972. Hydraulics of groundwater. New-York: McGraw-Hill.

Bouwer, H., 2002. Artificial recharge of groundwater: Hydrogeology and engineering. Hydrogeol. J. 10, 121–142.

Brown, C.J., 2005. Planning Decision Framework for Brackish Water Aquifer, Storage and Recovery (ASR) Projects. Ph.D. Thesis, University of Florida, Gainesville, FL, USA.

Burgéap., 1995. Etude de la nappe de l'Est Lyonnais - Paris : Ministère de l'environnement, Lyon (France) : Direction Départementale de l'Agriculture et de la Forêt du Rhône, 45 p+11 cartes

Chastanet J., Kaskassian S., Côme J.M., Malard F., Foulquier A., 2008 Transport de chaleur et température des nappes phréatiques à l'aplomb des bassins d'infiltration d'eau de ruissellement pluvial. Projet ANR-05-ECOT-006.

COMSOL Multiphysics Reference Manual, version 5.4", COMSOL, Inc, www.comsol.com

Darcy, H., 1856. Les Fontaines Publiques de la Ville de Dijon : Exposition et Application. Victor Dalmont, Paris, France

Datry, T., Malard, F., Gibert, J., 2004. Dynamics of solutes and dissolved oxygen in shallow urban groundwater below a stormwater infiltration basin. Sci. Total Environ. 329, 215–229.

Davis, A.P., Hunt, W.F., Traver, R.G., Clar, M., 2009. Bioretention technology: overview of current practice and future needs. J. Environ. Eng. 135, 109–117.

Dillon, P., 2005. Future management of aquifer recharge. Hydrogeol. J. 13, 313–316.

Eusuff, M.M., Lansey, K.E., 2004. Optimal operation of artificial groundwater recharge systems considering water quality transformations. Water Resour. Manag. 18, 379-405.

Foulquier, A., 2010. Élaboration d'un outil opérationnel pour la maitrise des impacts des ouvrages d'infiltration d'eau de ruissellement pluvial sur le régime thermique des nappes phréatiques. Rapport Final, ZABR, Lyon, France.

Goutaland, D., Winiarski, T., Dubé, J.-B., Bievre, G., Buoncristiani., J.-F., Chouteau, M., Giroux, B., 2008. Hydrostratigraphic Characterization of Glaciofluvial Deposits Underlying an Infiltration Basin Using Ground Penetrating Radar. Vadose zone. J. 7, 194-207.

Hunt, W., Traver, R., Davis, A., Emerson, C., Collins, K., Stagge, J., 2010. Low Impact Development Practices: Designing to Infiltrate in Urban Environments. Effects of urbanization on Groundwater: pp. 308–343

Bertrand-Krajewski, J.-L., Barraud, S., Gibert, J., Malard, F., Winiarski, T., Delolme, C., 2004. The OTHU case study: integrated monitoring of stormwater (Lyon, France). In: Unesco IHP-VI Data Requirements for Integrated Urban Water Management

Maliva, R.G., Guo,W., Missimer, T.M., 2006. Aquifer Storage and Recovery: Recent Hydrogeological Advances and System Performance. Water Environ. Res. 78, 2428–2435.

Mason, Y., Amman, A., Ulrich, A., Sigg, L., 1999. Behaviour of heavy metals nutrients and major components during roof runoff infiltration. Environ Sci Technol. 33,1588–1597.

Merritt, M.L., 1985. Subsurface Storage of Freshwater in South Florida: A Digital Model Analysis of Recoverability. Water Supply Paper 2261. U.S. Geological Survey: Alexandria, VA, USA.

Merritt, M.L., 1986. Recovering FreshWater Stored in Saline Limestone Aquifers. Ground Water. 24, 516–529.

Millington, R. J., Quirk, J. P., 1961. Transport in porous media [in soil science], Trans. Int. Congr. Soil Sci. 7(1), 97–106.

Minsley, B.J., Ajo-Franklin, J., Mukhopadhyay, A., Morgan, F.D., 2011. Hydrogeophysical Methods for Analyzing Aquifer Storage and Recovery Systems. Ground Water. 49, 250-269.

Mualem, Y., 1976. A new model for predicting the hydraulic conductivity of unsaturated porous media. Water Resour. Res. 12, 513-522.

Pinasseau, L., Wiest, L., Fildier, A., Volatier, L., Fones, G. R., Mills, G. A., Mermillod-Blondin, F., Vulliet, E., 2019. Use of passive sampling and high resolution mass spectrometry using a suspect screening approach to characterise emerging pollutants in contaminated groundwater and runoff. Sci. Total Environ. 672, 253-263.

Pitt, R., Clark, S., Field, R., 1999. Groundwater contamination potential from stormwater infiltration practice. Urban Water. 1, 217–236

Rahman, M.A., Rusteberg, B., Uddin, M.S., Lutz, A., Saada, M.A., Sauter, M., 2013. An integrated study of spatial multicriteria analysis and mathematical modelling for managed aquifer recharge site suitability mapping and site ranking at northern Gaza coastal aquifer. J. Environ. Manag. 124, 25-39.

Richards, L.A., 1931. Capillary conduction of liquids through porous mediums. Physics. 1, 318–333.

Ringleb, J., Sallwey, J., Stefan, C., 2016. Assessment of Managed Aquifer Recharge through Modeling- A Review. Water. 8, 579.

Slimene, E. B., Lassabatere, L., Šimůnek, J., Winiarski, T., Gourdon, R., 2017. The role of heterogeneous lithology in a glaciofluvial deposit on unsaturated preferential flow–a numerical study. Journal of Hydrology and Hydromechanics, 65(3), 209-221.

Tedoldi, D., Chebbo, G., Pierlot, D., Kovacs, Y., Gromaire, M.-C., 2016. Impact of runoff infiltration on contaminant accumulation and transport in the soil/filter media of sustainable urban drainage systems: a literature review. Sci. Total Environ. 569–570, 904–926.

Tutulic, M.R., Adams, K.N., Shamseldin, A.Y., Melville, B.W. Modelling aquifer recharge with stormwater in urban areas. 7th South Pacific Stormwater Conference, Auckland, New Zealand, 04-06 May (2011)

Tzoraki, O., Dokou, Z., Christodoulou, G., Gaganis, P., Karatzas, G., 2018. Assessing the efficiency of a coastal managed Aquifer Recharge (MAR) system in Cyprus. Sci. Total Environ. 626, 875-886.

Van Genuchten, M.Th., 1980. A closed form equation for predicting the hydraulic conductivity of unsaturated soils. Soil Sci. Soc. Am. J. 44, 892-898.

Voisin, J., Cournoyer, B., Vienney, A., & Mermillod-Blondin, F. (2018). Aquifer recharge with stormwater runoff in urban areas: Influence of vadose zone thickness on nutrient and bacterial transfers from the surface of infiltration basins to groundwater. Sci. Total Environ. 637, 1496-1507.

Winiarski, T., Lassabatere, L., Angulo-Jaramillo, R., Goutaland, D., 2013. Four decades of progress in monitoring and modeling of processes in soil-plant-atmosphere system: Application and Challenges. Procedia Environmental Sciences. 19, pp 955-964

Grenoble
March 14th, 2020

Conflicts of Interest Statement

The authors whose names are listed immediately below certify that they have NO affiliations with or involvement in any organization or entity with any financial interest (such as honoraria; educational grants; participation in speakers' bureaus; membership, employment, consultancies, stock ownership, or other equity interest; and expert testimony or patent-licensing arrangements), or non-financial interest (such as personal or professional relationships, affiliations, knowledge or beliefs) in the subject matter or materials discussed in this manuscript

Tidjani Bahar

Laurent Oxarango

Helene Castebrunet

Yvan Rossier

Florian Mermillod-Blondin